Research Square

Preprints are preliminary reports that have not undergone peer review.
They should not be considered conclusive, used to inform clinical practice,
or referenced by the media as validated information.

Influence of hooked-end steel fibres on the fresh and hardened properties of concrete using Dreux–Gorisse mix design method

NOUR-EDDINE OUSLIMANE

noureddine.ouslimane@uit.ac.ma

Hanane BAREBITA
Youssef MERROUN
Jaouad BENSALAH
Fouad DIMANE
Mustapha BELFAQUIR

Research Article

Keywords: Steel fibre, Reinforced concrete, Dreux-Gorisse, Method, Compressive strength, Workability, Aggregates

Posted Date: July 6th, 2026

DOI: https://doi.org/10.21203/rs.3.rs-10152203/v1

License: This work is licensed under a Creative Commons Attribution 4.0 International License.
Read Full License

Additional Declarations: No competing interests reported.

Version of Record: A version of this preprint was published at Discover Materials on October 24th, 2026. See the published version at https://doi.org/10.1007/s43939-026-01033-3.

Influence of hooked-end steel fibres on the fresh and hardened properties of concrete using Dreux–Gorisse mix design method

Nour-eddine OUSLIMANE[1,2*], Hanane BAREBITA[3,2], Youssef MERROUN[4], Jaouad BENSALAH[1], Fouad DIMANE[5], Mustapha BELFAQUIR[1].

[1] Laboratory of Advanced Materials and Process Engineering (LMAGP), Faculty of Sciences, University Ibn Tofail, BP 133, Kenitra, Morocco.

[2] Testing laboratory, Building and civil engineering testing and studies, TEST-BUILDING, Kenitra, Morocco.

[3] Organic Chemistry, Catalysis and Environment Laboratory, Chemistry Department, Faculty of Sciences, Ibn Tofail University, BP 133, Kenitra, Morocco.

[4] Laboratory of Organic, Organometallic and Theoretical Chemistry, Faculty of Science, University of IbnTofail, B.P. 133, 14000, Kenitra, Morocco

[5] National School of Applied Sciences of Al-Hoceima, Department of Energy and Environmental Civil Engineering, Engineering Sciences and Applications Laboratory, Abdelmalek Essaadi University, Tetouan, Morocco.

*Correspondence: noureddine.ouslimane@uit.ac.ma (NO)

Abstract

This study investigates the influence of hooked-end steel fibres on the fresh and hardened properties of concrete produced using locally sourced and fully characterised aggregates. The reference concrete mix was designed using the Dreux–Gorisse method to ensure a consistent grading approach and to minimise variability in mixture composition. The aggregates were evaluated through standard physical and mechanical tests, including particle size distribution, sand equivalent, flakiness index, Los Angeles abrasion, and bulk density. Three steel fibre dosages (20, 30, and 40 kg/m³) were incorporated into the control mix to assess their effect on workability, density, and compressive strength at 7 and 28 days. The results show a significant reduction in workability with increasing fibre content, with slump decreasing from 6.0 cm for the control mix to 1.5 cm at 40 kg/m³, corresponding to a 75% reduction. Conversely, hardened concrete density increased progressively due to the high intrinsic density of steel fibres. Compressive strength improved substantially with fibre addition, reaching a maximum increase of 32.7% at 28 days for the highest fibre dosage. This enhancement is attributed to crack-bridging mechanisms, improved stress transfer, and effective mechanical anchorage provided by the hooked-end geometry. The findings demonstrate that steel fibre reinforcement significantly enhances the mechanical performance of conventional concrete while maintaining acceptable workability when properly

controlled. The use of a single, well-defined mix design enabled the isolation of fibre effects, providing a robust framework for performance evaluation in infrastructure materials.

Keywords: Steel fibre, Reinforced concrete, Dreux-Gorisse, Method, Compressive strength, Workability, Aggregates.

1. Introduction

Concrete is the most widely used construction material worldwide due to its availability and mechanical performance. Initially composed of four basic constituents—coarse aggregates, sand, cement, and water— its formulation has progressively evolved from an empirical practice to a discipline grounded in materials science to a discipline grounded in materials science [1–5]. Its widespread use is attributed to low production cost, the accessibility of its raw materials, and excellent compressive performance [6–8]. However, concrete exhibits inherently low tensile strength and brittle fracture behaviour upon crack initiation, limiting its capacity to dissipate energy and arrest crack propagation. As a result, conventional steel reinforcement remains indispensable to ensure structural safety and durability [9,10].

Among the strategies proposed to overcome these limitations, the incorporation of fibres into the cementitious matrix has emerged as one of the most effective approaches [11–14]. When homogeneously distributed throughout the mix, fibres act as three-dimensional reinforcement capable of restraining microcrack initiation and propagation [15,16]. This reinforcement mechanism improves ductility, toughness, fatigue resistance, and post-cracking behaviour [17,18]. Steel fibres are particularly suited to structural applications owing to their high elastic modulus, excellent bond with the cement paste, and tensile strength exceeding 1000 MPa, in accordance with standard NF EN ISO 16120-2 [19–21].

Over the past several decades, numerous studies have examined the influence of steel fibres on the fresh and hardened properties of concrete [22–24]. It is consistently reported that fibre incorporation reduces workability due to the increased specific surface area of the mix and the mechanical interlocking between fibres, often necessitating adjustment of the water-to-cement ratio or the use of superplasticisers [25,26]. Conversely, mechanical performance is significantly improved through crack-bridging action, which promotes more effective stress transfer and delays brittle failure [27,28]. Several authors report compressive strength gains ranging from 27% to 40% for fibre contents between 20 and 40 kg/m³ [29,30], while others highlight the critical influence of fibre geometry, aspect ratio, and anchorage type on the final mechanical behaviour [31].

Despite these promising findings, comparisons across studies remain challenging owing to considerable differences in mix design, notably in fibre content, superplasticiser dosage, water-to-cement ratio, and aggregate nature [32,33]. This variability complicates the isolation of the specific effect of fibres on concrete performance. Furthermore, aggregates are not always subjected to thorough physical and mechanical characterisation prior to their use, despite exerting a strong influence on concrete

performance and durability [34,35]. This heterogeneity represents a significant limitation in interpreting and comparing results reported in the literature [36].

In this context, the present study aims to rigorously evaluate the influence of hooked-end steel fibre content on the physical and mechanical properties of concrete produced from previously characterised local aggregates [37,38]. In contrast to many prior investigations, a single reference mix formulated by the Dreux-Gorisse method was consistently applied across all batches in order to isolate the exclusive effect of fibre dosage [39,40].

The specific objectives of this study are: (i) to characterise local aggregates through standardised testing; (ii) to design a reference concrete mix using the Dreux-Gorisse method; and (iii) to evaluate the influence of four hooked-end steel fibre dosages (0, 20, 30, and 40 kg/m³) on workability, bulk density, and compressive strength at 7 and 28 days.

2. Materials and Experimental Methods

2.1 Experimental Framework

All tests were conducted at the TEST-BUILDING Laboratory, an accredited testing facility operational since 2003 and a key actor in quality control in the construction and civil engineering sectors in Morocco. The laboratory is active in geotechnical investigations, materials testing, structural modelling, and applied research on locally available materials.

2.2 Materials

All concrete constituents were sourced locally. Table 1 summarises the materials used and their principal characteristics.

Table 1 Materials used in concrete production and their characteristics

Component	Description	Standard
Cement	CEM I 42.5 R — Ordinary Portland Cement 	NF EN 197-1
Sea sand (SS)	Sand 0/0.8 mm — MF = 1.08 	NM EN 933-1

	Sand 0/6.3 mm — MF = 2.92	
Crushed sand (CS)		NM EN 933-1
	Gravier (GI) 6.3/14 mm	
Coarse aggregate GI		NM EN 933-1
	Gravier (GII) 10/20 mm	
Coarse aggregate GII		NM EN 933-1
	Hooked-end steel fibres l = 30-60 mm, Ø = 0,5-1,3 mm, Rt > 1000 MPa	
Steel fibres		NF EN ISO 16120-2

The steel fibres employed are of the hooked-end type, a geometry that maximises mechanical anchorage within the cementitious matrix. They were introduced directly into the mixing water prior to blending to ensure homogeneous dispersion and prevent fibre balling (hedgehog effect).

2.3 Aggregate Characterisation

A comprehensive series of standardised tests was performed on all aggregates to determine their physical, geometric, and mechanical characteristics. These results constitute the input data for the concrete mix design procedure.

2.3.1 Particle Size Analysis

Particle size analysis was conducted by passing aggregate samples through a nest of sieves with decreasing aperture sizes (from 80 mm to 0.063 mm) in accordance with standard NM EN 933-1 [41]. The results were used to plot grading curves for each constituent and to calculate the fineness modulus (FM) of the sands using:

$$FM = \frac{1}{100}\sum(\text{cumulative retained percentages on selected sieves})$$

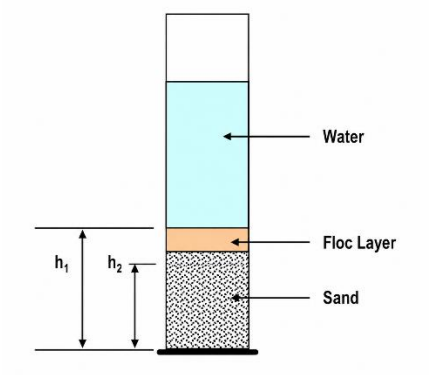
Results:

- FM (sea sand) = 1.08
- FM (crushed sand) = 2.92
- Combined sand FM ≈ 2.00 (optimal for Dreux–Gorisse method)

2.3.2 Sand Equivalent Test

The sand equivalent (SE) test assesses the cleanliness of sands with respect to clay fines. It involves agitating a sand sample (fraction 0/2 mm) in a flocculating solution, then measuring the height of the sediment (h_2) and the flocculate (h_1) in accordance with standard NM EN 933-8 [42]. The sand equivalent is calculated as:

$$\mathbf{SE(10\%)} = \frac{\mathbf{H_2}}{\mathbf{H_1}}\mathbf{100}$$



where $\mathbf{h_1}$ is the total height (sediment + flocculate) and $\mathbf{h_2}$ is the height of the sediment alone.

Results obtained were: SE (crushed sand) = 89% and SE (sea sand) = 50%. The crushed sand is classified as 'very clean' (SE > 85%), whereas the sea sand, with SE below the recommended threshold of 65%, indicates a potentially problematic clay fines content requiring pre-washing before use.

2.3.3 Flatness Index

This test determines the proportion of flat or elongated particles in a coarse aggregate by successive sieving through square-mesh sieves followed by bar sieves, in accordance with standard NM EN 933-3 [43] in Table 2. The flatness index (Fl) is given by:

$$FI = \frac{M_2}{M_1}\ \mathbf{100}$$

Where $\mathbf{M_1}$ is the total mass of the tested fraction and $\mathbf{M_2}$ is the mass of particles passing through the bar sieve.

Table 2 Flatness index of coarse aggregates

Aggregate Class	GI 6.3/14 mm	GII 10/20 mm
Fl (%)	15	13

Results indicate Fl (GI) = 15% and Fl (GII) = 13%, satisfactory values attesting to aggregate shapes approaching cubic or spherical geometry, which is favourable to achieving high concrete compactness.

2.3.4 Surface Cleanliness

Surface cleanliness measures the percentage of fine particles (< 0.5 mm) adhering to the surface of coarse aggregates, in accordance with standard NM 10.1.169 [44]. It is expressed as:

$$P = \frac{m}{M_s}\ 100$$

where M_s **:** is the dry mass of the test specimen and **m** is the mass of particles smaller than 0.5 mm.

Results were: P (GI) = 0.8% and P (GII) = 0.6%, both very low values confirming the good surface quality of the aggregates.

2.3.5 Bulk Density

Bulk density was determined by weighing aggregates filling a container of known volume, in accordance with standard NM EN 1097-3 [45]. Mean values obtained are presented in Table 3.

Table 3 Bulk density of aggregates

Aggregate	Mvapp		Mean (Mg/m³)
	Trial 1 (Mg/m³)	Trial 2 (Mg/m³)	
GI (6.3/14 mm)	1.40	1.40	1.40
GII (10/20 mm)	1.39	1.41	1.40
Sea sand	1.35	1.37	1.36
Crushed sand	1.36	1.40	1.38

2.3.6 Los Angeles Abrasion Test

The Los Angeles test measures the resistance of aggregates to fragmentation by impact and friction in a rotating drum, in accordance with standard NM EN 1097-2 [46]. The Los Angeles coefficient is computed as:

$$L_A = \frac{m}{M} \times 100$$

Where **M** is the initial mass of the test sample and **m** is the mass of material passing the 1.6 mm sieve after testing.

Results were: LA (GI) = 24% and LA (GII) = 21%. Both values below 30% classify the coarse aggregates as mechanically sound and suitable for structural concrete production.

2.4 Concrete Mix Design — Dreux-Gorisse Method

The Dreux-Gorisse method was applied to determine the optimal proportions of concrete constituents per cubic metre [47]. This method is based on constructing a reference grading curve OXY that identifies the aggregate combination with minimum void content in Figure 1.

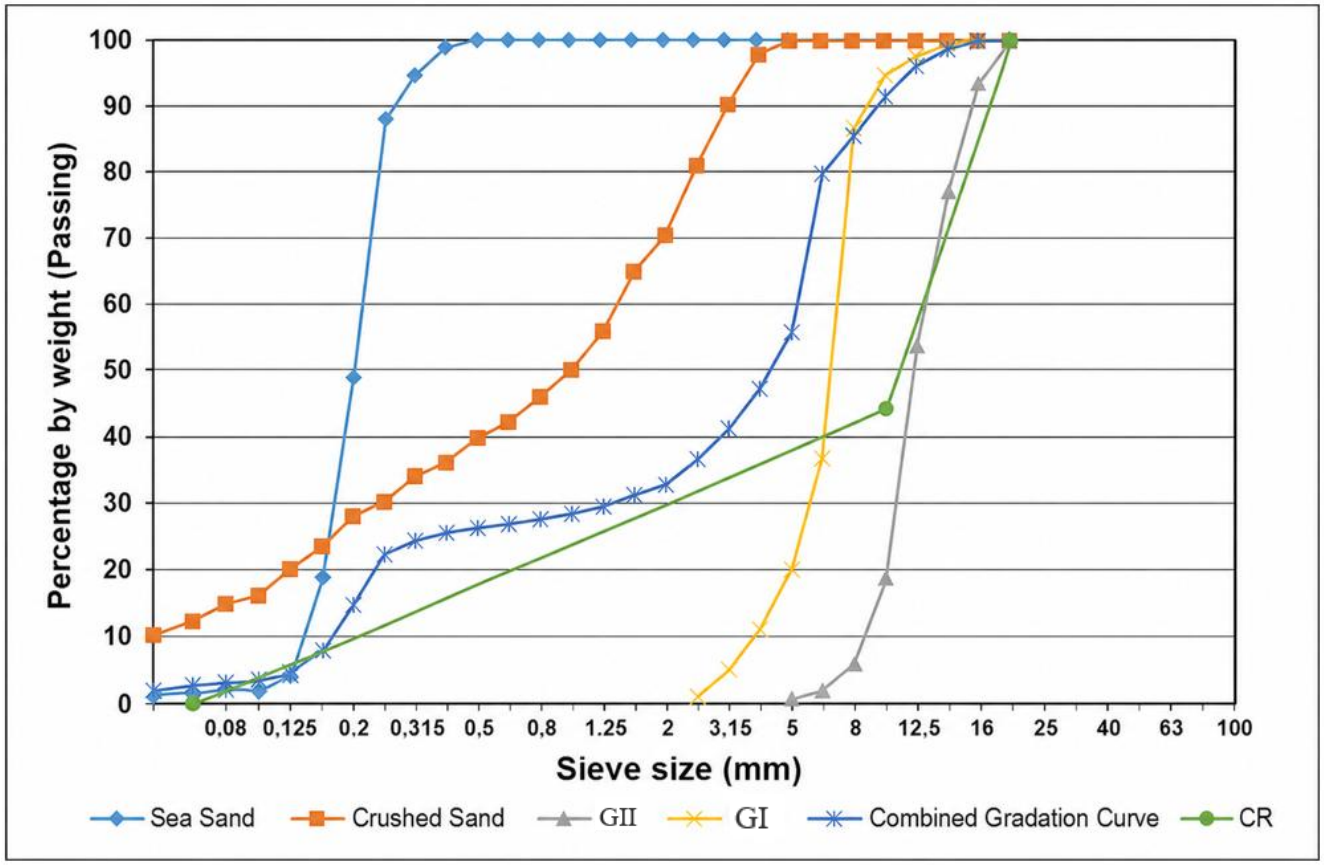


Fig. 1 Reference grading curve — Dreux-Gorisse method

Key parameters of the reference curve:

- **Dmax** = 20 mm → Breakpoint X = 10 mm
- Mean fineness modulus FM = 2.00
- $\boldsymbol{K = K + K_s}$ = 2 + (6 × 2.00 − 15) = −1
- $\boldsymbol{Y_A = 50 - \sqrt{D_{max}} + KA}$ = 50 − √20 + (−1) = 44.52%

The reference grading curve yielded the following optimal proportions for each aggregate class:

- Sand blend: 34%

- Coarse aggregate 10/20: 58%
- Coarse aggregate 6.3/14: 8%

The final reference concrete composition is summarised in Table 4.

Table 4 Reference concrete composition — Dreux-Gorisse method (kg/m³)

Component	**Dosage per 1m³**		Volumetric composition for 1 bag of cement (L)
	(Kg)	(L)	
Coarse aggregate 10/20	1087	776	110
Coarse aggregate 6.3/14	149	105	15
Sea sand	315	228	33
Crushed sand	311	229	33
Cement	350	112	50
Water (L)	166		24
W/C ratio	0.47		*****
Theoretical density (kg/m³)	2380		*****

A water-to-cement ratio of 0.47 is consistent with a target 28-day compressive strength of 25 to 30 MPa according to the Bolomey equation. This mix constitutes the control concrete (CC) to which steel fibres were added in subsequent batches.

2.5 Steel Fibre Incorporation

Three hooked-end fibre dosages were examined as additions to the reference mix composition: 20, 30, and 40 kg/m³. The corresponding fibre quantities per 160 × 320 mm cylindrical specimen are 128 g, 193 g, and 257 g, respectively. Fibres were introduced directly into the mixing water prior to blending to ensure homogeneous distribution and to prevent fibre clumping (balling).

2.6 Testing Programme

2.6.1 Slump Test (Abrams Cone)

Fresh concrete workability was assessed using the Abrams cone (height: 300 mm, base diameter: 200 mm, top diameter: 100 mm). Concrete was placed in three equal layers, each rodded 25 times, in accordance with standard NM 10.1.061 [48,49]. The slump was measured immediately after demoulding, to the nearest 10 mm in Figure 2.



Fig. 2 Abrams cone slump test

2.6.2 Bulk Density of Hardened Concrete

The bulk density of hardened concrete was determined on 160 × 320 mm cylindrical specimens at 7 and 28 days, in accordance with standard NM 10.1.065 [50,51] in Figure 3. Specimen volume was calculated as

$$\boldsymbol{V = \pi \times \frac{D^2}{4} \times h}$$



Fig. 3 Weighing of hardened concrete specimen for density determination

For a cylinder of **160 mm** × **320 mm**:

$$\mathbf{V} = \pi \times \frac{160^2}{4} \times 320$$

$$\mathbf{V} = 6\,434\,000\ mm^3$$

$$\mathbf{V} = 6434\ cm^3$$

2.6.3 Compressive Strength

Specimens were cured for 24 hours in their moulds, then immersed in a water bath maintained at 21–23 °C until the test age (7 and 28 days), in accordance with standard NM 10.1.051 [52,53]. Three specimens per age and per formulation were tested under uniaxial compression. The reported values correspond to the average of three specimens and the standard deviation was calculated in Figure 4 and 5.

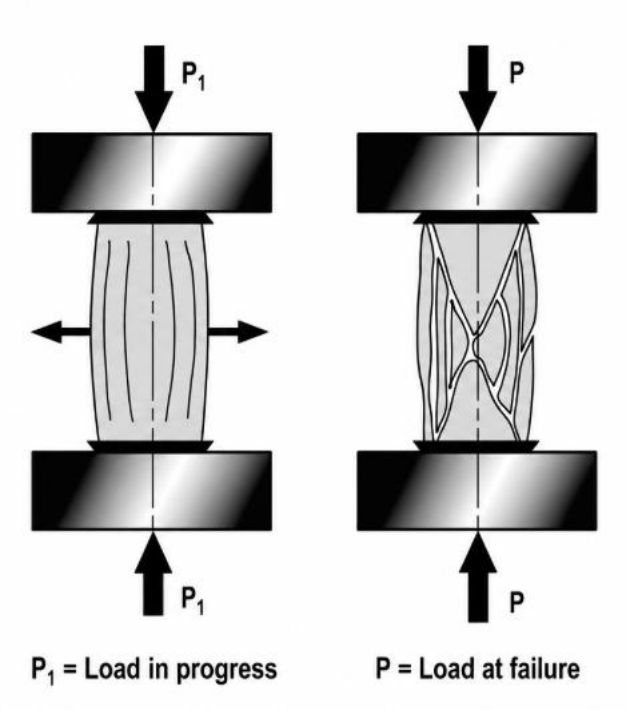


Fig.4 Application of compressive load on a cylindrical specimen

Compressive strength was calculated as:

$$\mathbf{Rc} = \frac{\mathbf{F}}{\mathbf{S}}$$

Where:

- **Rc** is the compressive strength (MPa),
- **F** is the maximum load (N),
- **S** is the cross-sectional area of the specimen (mm^2) calculated from its nominal diameter.

Results are reported to the nearest 0.5 MPa.



Fig.5 Failure mode of a cylindrical specimen under compressive loading

3. Results and Discussion

3.1 Aggregate Characterisation

Table 5 summarises all physical and mechanical properties of the aggregates determined during the testing campaign. These data served as input parameters for the concrete mix design.

Table 5 Summary of aggregate properties

Property	Unit	GI (6.3/14)	GII (10/20)	Crushed sand	Sea sand
Maximum size Dmax	mm	14	20	6,3	0,8
Fineness Modulus FM	%	—	—	2.92	1.08
Sand Equivalent SE	%	—	—	89	50
Flatness Index Fl	%	15	13	—	—
Surface Cleanliness P	%	0.8	0.6	—	—
Bulk Density	Mg/m^3	1.40	1.40	1.38	1.36
Los Angeles Coefficient LA	%	24	21	—	—

All aggregates exhibited characteristics consistent with structural concrete production. The Los Angeles coefficient below 25% for GII indicates excellent resistance to fragmentation. The sea sand equivalent (SE = 50%) falls below the recommended threshold (SE > 65%) and was therefore pre-washed prior to use. The crushed sand, with SE = 89%, is classified as very clean.

3.2 Workability

Slump tests were performed on all four concrete mixes. Results are presented in Table 6 and Figure 6.

Table 6 Slump test results

Parameter	0 (control)	20	30	40
Slump A (cm)	6.0±0.2	3.0±0.2	2.5±0.2	1.5±0.1
Consistency Class	S2	S1	S1	S1

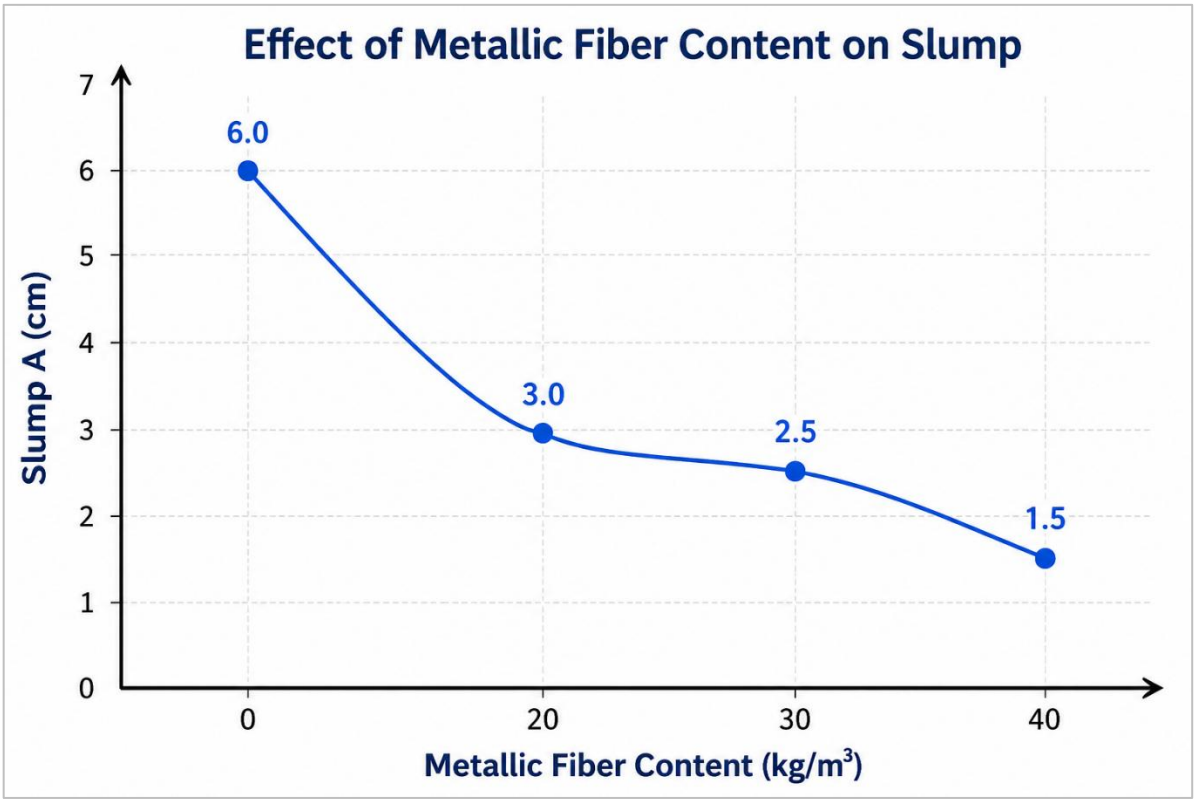


Fig. 6 Effect of fibre content on fresh concrete workability.

Steel fibre incorporation induced a significant and progressive reduction in workability. The slump decreased from 6.0 cm for the control mix to 1.5 cm at 40 kg/m³, representing a 75% reduction. This loss of workability is attributed to two principal mechanisms: the increased total specific surface area of the fibres, which absorbs a portion of the mixing water, and the mechanical bridging action of fibres that resists concrete flow. The higher the fibre aspect ratio (length-to-diameter), the more pronounced this effect. The maximum slump loss observed was 4.5 cm (75%), which remains manageable in practice through the addition of a superplasticiser.

3.3 Bulk Density of Hardened Concrete

The evolution of mean concrete bulk density as a function of fibre dosage and curing age is presented in Table 7 and Figure 7.

Table 7 Mean bulk density of hardened concrete for different steel fibre contents.

Fibre Content (kg/m³)	Density at 7 days (g/cm³)	Density at 28days (g/cm³)
0 (control)	2.34±0.01	2.36±0.01
20	2.39±0.02	2.40±0.02
30	2.44±0.03	2.45±0.03
40	2.50±0.04	2.53±0.04

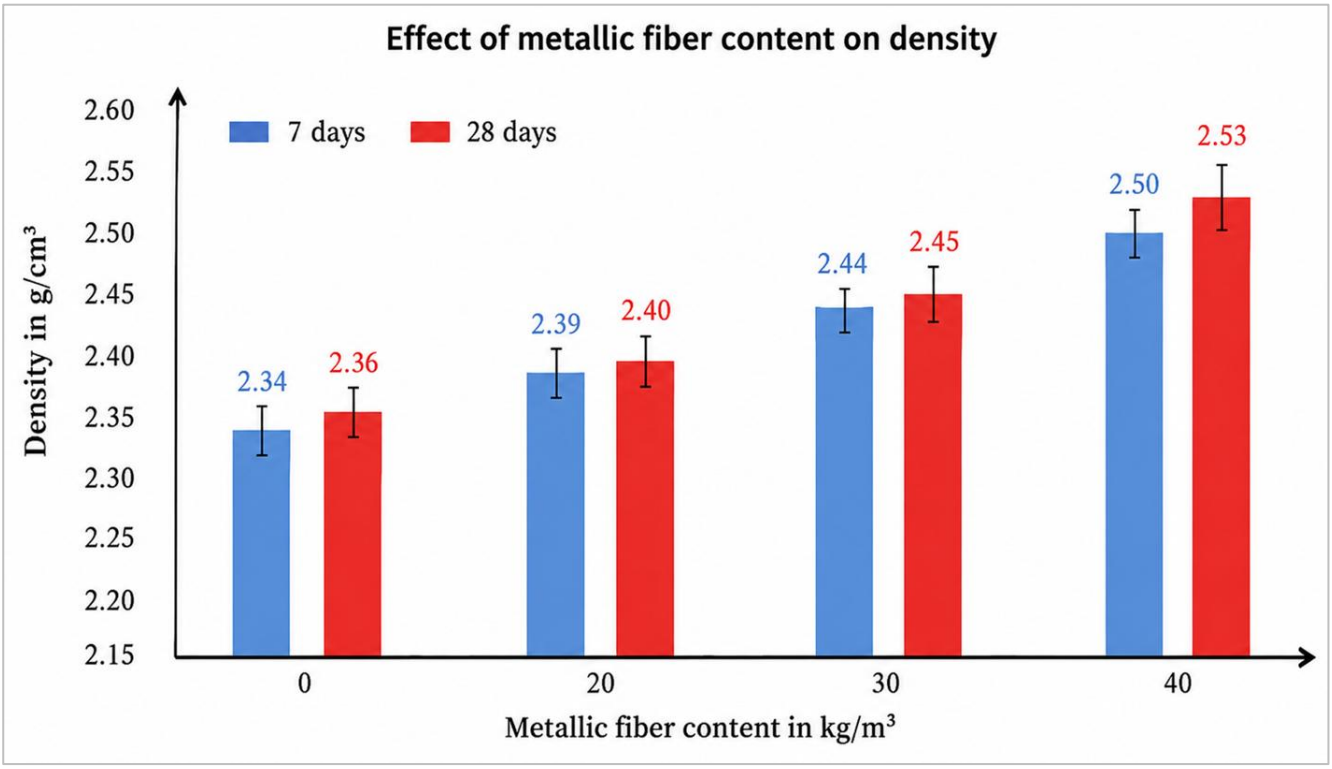


Fig. 7 Evolution of bulk density as a function of fibre content

Bulk density increased steadily with increasing fibre content. This trend is directly attributable to the intrinsic density of steel ($\rho \approx 7.8$ g/cm³), which is substantially higher than that of plain concrete (≈ 2.35 g/cm³). A positive correlation was observed between bulk density and compressive strength, confirming that fibres contribute to densifying the cementitious matrix. The marginal increase in density between 7 and 28 days reflects the continued progression of cement hydration.

3.4 Compressive Strength

Compression tests were conducted at 7 and 28 days on three specimens per mix. Mean results are presented in Table 8 and Figure 8.

Table 8 Compressive strength as a function of fibre content and curing age

Fibre Content (kg/m³)	Compressive Strength (MPa)	
	Rc 7 days	Rc 28 days
0 (control)	19.5±0.2	26.0±0.5
20	20.0±0.3	28.0±0.4
30	23.0±0.4	31.0±0.6
40	25.5±0.5	34.5±0.7

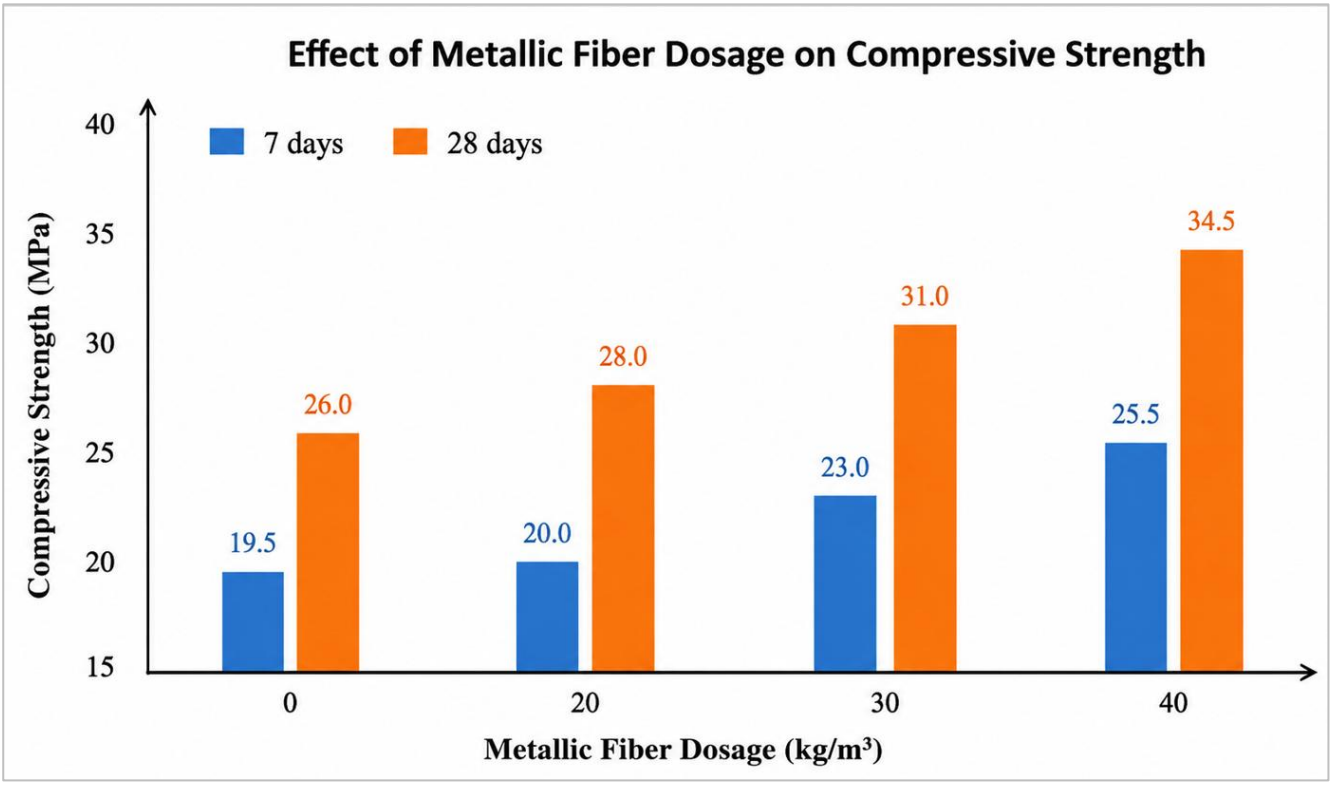


Fig.8 Relative compressive strength gains relative to the control mix

Results reveal a systematic and progressive improvement in compressive strength with increasing fibre content. At 28 days, the maximum gain of 32.7% was achieved at 40 kg/m³, while a dosage of 30 kg/m³ yielded a gain of 19.2%. Even at the lowest dosage of 20 kg/m³, a gain of 7.7% was recorded relative to the control mix at 28 days.

4. Discussion

The mechanical improvement observed in compressive strength can be attributed to three principal reinforcement mechanisms:

- ✓ Hooked-end steel fibres provide enhanced mechanical anchorage due to their geometry, significantly increasing the pullout force.
- ✓ The fibres act as crack-bridging elements that delay crack initiation and propagation, slowing down the progressive breakdown of the cement matrix.
- ✓ Multidirectional fiber reinforcement improves the mechanical isotropy of concrete by distributing stresses in all directions.

The effect of fibres in compression, although positive, remains less than that observed in tension or bending, because compression cracks generate tangential movements which stress the fibres in shear, a condition less favourable to the full mobilization of their mechanical capacities.

The results further confirm the effectiveness of the Dreux-Gorisse method as a robust and reproducible mix design protocol for locally sourced aggregates. The use of a single reference mix formulation across all test series allowed the fibre effect to be isolated with a high degree of scientific rigour, which represents a methodological advantage over many comparative studies reported in the literature.

5. Conclusions

This study evaluated the effect of hooked-end steel fibres on the fresh and hardened properties of concrete designed using the Dreux–Gorisse method and locally sourced aggregates. The results demonstrated that fibre incorporation significantly enhanced concrete performance while affecting its workability.

The addition of steel fibres reduced slump from 6.0 cm to 1.5 cm as the fibre dosage increased from 0 to 40 kg/m³, indicating a decrease in workability due to increased internal friction and fibre interlocking. Conversely, hardened concrete density and compressive strength increased with fibre content.

The optimum fibre dosage was found to be 40 kg/m³, which resulted in a 32.7% increase in compressive strength while maintaining acceptable workability. This dosage may therefore be recommended for structural concrete applications requiring enhanced crack resistance and mechanical performance.

The observed improvement is mainly attributed to the crack-bridging action of the fibres and the efficient mechanical anchorage provided by their hooked-end geometry, which delays crack propagation and enhances stress transfer within the cementitious matrix. These findings confirm that hooked-end steel fibres are an effective solution for improving the mechanical behaviour of conventional concrete produced with local materials.

Further studies should investigate tensile and flexural behaviour, post-cracking performance, and long-term durability in order to provide a more comprehensive assessment of steel fibre reinforced concrete for structural applications**.**

Declarations

Ethics approval and consent to participate

Not applicable.

Clinical Trial Registration

Not applicable. This study is not a clinical trial; it is a materials science investigation on concrete properties. No clinical trial registration is required.

Conflicts of Interest

The authors report that there are no conflicts of interest relevant to this research work.

Funding Statement

There is no funding to report for this submission.

Data availability statement

All data generated or analyzed during this study are provided in full within the published article.

References

[1] P.C. Aïtcin, R.J. Flatt, Science and Technology of Concrete Admixtures, Constr. Build. Mater. 368 (2023) 130432. https://doi.org/10.1016/j.conbuildmat.2023.130432

[2] A. Mohammed, S. Rafiq, W. Mahmood, et al., Physico-mechanical properties of sustainable concrete incorporating local waste materials, Case Stud. Constr. Mater. 14 (2021) e00494. https://doi.org/10.1016/j.cscm.2021.e00494

[3] P.K. Mehta, P.J.M. Monteiro, Microstructure and Properties of Hardened Concrete, Constr. Build. Mater. 249 (2020) 118795. https://doi.org/10.1016/j.conbuildmat.2020.118795

[4] R. Sharma, A. Jain, N. Gupta, Evolution of concrete mix design methods: a critical review, Mater. Today Proc. 65 (2022) 1234–1241. https://doi.org/10.1016/j.matpr.2022.04.512

[5] A. Bentur, S. Mindess, Fibre Reinforced Cementitious Composites, Constr. Build. Mater. 223 (2019) 811–820. https://doi.org/10.1016/j.conbuildmat.2019.06.118

[6] N.T. Tran, D.J. Kim, M.K. Kim, Effect of steel fiber content on the compressive behavior of ultra-high-performance concrete, Constr. Build. Mater. 272 (2021) 121928. https://doi.org/10.1016/j.conbuildmat.2020.121928

[7] J. He, W. Chen, B. Zhang, et al., The mechanical properties and damage evolution of UHPC reinforced with glass fibers and steel fibers, Constr. Build. Mater. 245 (2020) 118457. https://doi.org/10.1016/j.conbuildmat.2020.118457

[8] P. Zhang, C. Wang, J. Wu, et al., Mechanical properties of steel fiber-reinforced concrete (SFRC) under repeated impact loading, J. Build. Eng. 56 (2022) 104893. https://doi.org/10.1016/j.jobe.2022.104893

[9] X. Liu, T. Wu, X. Yang, et al., Properties of self-compacting lightweight aggregate concrete reinforced with steel and polypropylene fibers, Constr. Build. Mater. 233 (2020) 117340. https://doi.org/10.1016/j.conbuildmat.2019.117340

[10] B.T. Huang, J.Q. Wu, J. Yu, et al., Seawater sea-sand engineered/strain-hardening cementitious composites (ECC/SHCC): assessment and modeling of crack characteristics, Cem. Concr. Res. 140 (2021) 106292. https://doi.org/10.1016/j.cemconres.2020.106292

[11] D.Y. Yoo, N. Banthia, Mechanical and structural behaviors of ultra-high-performance fiber-reinforced concrete subjected to impact and blast, Constr. Build. Mater. 149 (2019) 416–431. https://doi.org/10.1016/j.conbuildmat.2017.05.136

[12] J. Zhao, J. Liang, L. Chu, F. Yan, Experimental study on compressive strength of steel fiber-reinforced concrete under high temperature, Materials 12 (2019) 2607. https://doi.org/10.3390/ma12162607

[13] S.T. Deresa, J. Xu, F. Liao, et al., Mechanical properties and shrinkage of ECC containing industrial and recycled components under different curing conditions, J. Clean. Prod. 308 (2021) 127360. https://doi.org/10.1016/j.jclepro.2021.127360

[14] M. Nili, A. Azarioon, S.M. Hosseinian, Experimental study on effects of blast-furnace slag and silica fume with steel fibers on mechanical properties of concrete, Constr. Build. Mater. 253 (2020) 119193. https://doi.org/10.1016/j.conbuildmat.2020.119193

[15] X. Lv, Z. Yu, G. Ye, Quantitative analysis of crack propagation in concrete under uniaxial compression: a review, Theor. Appl. Fract. Mech. 123 (2023) 103704. https://doi.org/10.1016/j.tafmec.2022.103704

[16] Y. Wang, S. Chen, Y. Li, S. Hu, Cracking behavior of steel fiber-reinforced concrete beams under flexural loading: an experimental and numerical study, Eng. Fract. Mech. 268 (2022) 108441. https://doi.org/10.1016/j.engfracmech.2022.108441

[17] A.E. Naaman, H.W. Reinhardt, High performance fiber reinforced cement composites (HPFRCC): extended definition and shift in research emphasis, ACI Mater. J. 120 (2023) 45–56. https://doi.org/10.14359/51738823

[18] V. Li, S. Wang, Flexural behaviors of glass fiber-reinforced polymer (GFRP)-concrete hybrid systems, Compos. Part B Eng. 236 (2022) 109816. https://doi.org/10.1016/j.compositesb.2022.109816

[19] C. Zhang, M. Cao, L. Li, C. Chen, Reinforcing mechanism of hybrid steel fiber on mechanical properties of mortar under different curing ages, Materials 14 (2021) 5323. https://doi.org/10.3390/ma14185323

[20] Q. Dai, R. Si, Y. Huang, Mixture design and performance evaluation of SBS modified asphalt mixtures with steel fiber reinforcement, J. Clean. Prod. 259 (2020) 120888. https://doi.org/10.1016/j.jclepro.2020.120888

[21] H.A.S.A. El-Mal, A.S. Sherbini, H.E.M. Sallam, Mode II fracture toughness of hybrid FRCs, Int. J. Concr. Struct. Mater. 16 (2022) 14. https://doi.org/10.1186/s40069-022-00507-x

[22] N. Banthia, F. Majdzadeh, J. Wu, V. Bindiganavile, Fiber synergy in hybrid fiber reinforced concrete (HyFRC) in flexure and direct shear, Cem. Concr. Compos. 48 (2022) 91–97. https://doi.org/10.1016/j.cemconcomp.2013.10.018

[23] M.A. Köroğlu, The effects of steel fiber reinforcement on mechanical properties of concrete, Comput. Concr. 23 (2019) 215–222. https://doi.org/10.12989/cac.2019.23.4.215

[24] J. Han, M. Zhao, J. Chen, X. Lan, Effects of steel fiber length and coarse aggregate maximum size on mechanical properties of steel fiber reinforced concrete, Constr. Build. Mater. 209 (2019) 577–591. https://doi.org/10.1016/j.conbuildmat.2019.03.086

[25] A.I. El-Kassas, A.A.A. Hassan, Influence of hooked-end steel fiber dosage on fresh and hardened properties of low cement content self-consolidating concrete, Constr. Build. Mater. 263 (2020) 120561. https://doi.org/10.1016/j.conbuildmat.2020.120561

[26] S. Yehia, A. Douba, O. Abdullahi, S. Farrag, Mechanical and durability evaluation of fiber-reinforced self-compacting concrete, Constr. Build. Mater. 144 (2021) 560–571. https://doi.org/10.1016/j.conbuildmat.2017.03.228

[27] J. Bao, S. Li, P. Zhang, et al., Influence of the incorporation of recycled coarse aggregate on water absorption and chloride penetration into concrete, Constr. Build. Mater. 239 (2020) 117845. https://doi.org/10.1016/j.conbuildmat.2019.117845

[28] Z. Deng, X. Liu, X. Yang, et al., A study of tensile and compressive properties of hybrid basalt-polypropylene fiber-reinforced concrete under uniaxial loads, Struct. Concr. 22 (2020) 396–410. https://doi.org/10.1002/suco.201900324

[29] J.A.O. Barros, J.A. Figueiras, Flexural behavior of SFRC: testing and modeling, J. Mater. Civ. Eng. 11 (2019) 331–339. https://doi.org/10.1061/(ASCE)0899-1561(1999)11:4(331)

[30] O. Bonneau, M. Lachemi, E. Dallaire, et al., Mechanical properties and durability of two industrial reactive powder concretes, ACI Mater. J. 94 (2021) 286–292. https://doi.org/10.14359/295

[31] W. Pansuk, T.N. Nguyen, Y. Sato, et al., Shear capacity of high-performance fiber reinforced concrete I-beams, Constr. Build. Mater. 157 (2020) 182–193. https://doi.org/10.1016/j.conbuildmat.2017.09.057

[32] J. Kheir, A. Loukili, A.M. Soliman, M. Nehdi, Mechanical properties of concrete incorporating recycled glass: a comprehensive review, J. Clean. Prod. 253 (2020) 119823. https://doi.org/10.1016/j.jclepro.2019.119823

[33] S.I. Mohammed, K.B. Najim, Mechanical strength, flexural behavior and fracture energy of recycled concrete aggregate self-compacting concrete, Structures 23 (2020) 34–43. https://doi.org/10.1016/j.istruc.2019.10.015

[34] Q. Liu, L. Li, I.C. Ihekwaba, X. Liu, Effect of aggregate characteristics on the mechanical properties of concrete, Constr. Build. Mater. 295 (2021) 123623. https://doi.org/10.1016/j.conbuildmat.2021.123623

[35] E. Dong, X. Yu, W. Tian, et al., Study of concrete mixture design and mechanical performance with different aggregate types, Materials 15 (2022) 3138. https://doi.org/10.3390/ma15093138

[36] C. De Wolf, F. Yang, J. Cox, et al., Database of embodied quantity outputs: lowering material impacts through engineering, J. Archit. Eng. 26 (2020) 04020026. https://doi.org/10.1061/(ASCE)AE.1943-5568.0000408

[37] M. Rafieizonooz, J. Mirza, M.R. Salim, et al., Investigation of river sand and manufactured sand as fine aggregates in concrete, Constr. Build. Mater. 113 (2021) 294–306. https://doi.org/10.1016/j.conbuildmat.2016.03.032

[38] K. Chandramouli, P.S. Rao, N. Pannirselvam, et al., Strength properties of glass fiber concrete, ARPN J. Eng. Appl. Sci. 5 (2019) 1–5. https://doi.org/10.1016/j.conbuildmat.2019.116972

[39] N. Bouzoubaa, M. Lachemi, Self-compacting concrete incorporating high volumes of class F fly ash: preliminary results, Cem. Concr. Res. 31 (2020) 413–420. https://doi.org/10.1016/S0008-8846(00)00504-4

[40] M. Siline, A. Ezzerrouqi, M. Diouri, O. Sassi, Comparative study of concrete mix design methods applied to local materials in Morocco, J. Build. Eng. 64 (2023) 105643. https://doi.org/10.1016/j.jobe.2022.105643

[41] M. Yaghoubi, A. Hamidi, E. Ghasemi, Effect of recycled glass powder on the geotechnical properties of clay soils, Constr. Build. Mater. 293 (2021) 123517. https://doi.org/10.1016/j.conbuildmat.2021.123517

[42] X. Liu, Y. Ni, Q. Li, et al., Comprehensive analysis on the sand equivalent test and development of automated testing device for fine aggregate quality, Constr. Build. Mater. 342 (2022) 128043. https://doi.org/10.1016/j.conbuildmat.2022.128043

[43] W. Cao, Y. Zhang, H. Li, et al., Influence of aggregate flakiness on the workability and mechanical properties of concrete mixtures, Materials 14 (2021) 6035. https://doi.org/10.3390/ma14206035

[44] Z.H. Ou, B. Ma, S.W. Jian, Influence of sand particle size and content on performance of cement mortar and concrete, J. Wuhan Univ. Technol. Mater. Sci. Ed. 34 (2019) 952–960. https://doi.org/10.1007/s11595-019-2148-z

[45] A.K.H. Kwan, M. McKinley, Packing and film thickness theories for the mix design of high-performance concrete, J. Zhejiang Univ. Sci. A 15 (2018) 256–268. https://doi.org/10.1631/jzus.A1300278

[46] E. Muñoz, M. García-Casals, M. Xalabarder, Aggregate quality assessment for structural concrete: an integrated approach, Constr. Build. Mater. 210 (2019) 289–298. https://doi.org/10.1016/j.conbuildmat.2019.03.144

[47] A.A. Elhakam, A.E. Ahmed, A. Awad, Influence of self-healing, mixing method and adding silica fume on mechanical properties of recycled aggregates concrete, Constr. Build. Mater. 35 (2019) 421–427. https://doi.org/10.1016/j.conbuildmat.2012.04.013

[48] R. Wang, X. Gao, Relationship between flowability, bleed water and strength of cement paste with nano-SiO2, Nanomaterials 9 (2019) 85. https://doi.org/10.3390/nano9010085

[49] K.A. Mohd Sari, S.Z. Samsuddin, L.Y. Loon, et al., Effect of water-to-cement ratio on workability and compressive strength of concrete with plasticizer, IOP Conf. Ser. Mater. Sci. Eng. 1176 (2021) 012022. https://doi.org/10.1088/1757-899X/1176/1/012022

[50] M.G. Sohail, B. Wang, A. Jain, et al., Advancements in environmentally sustainable technologies for concrete durability: a review, Constr. Build. Mater. 308 (2021) 125021. https://doi.org/10.1016/j.conbuildmat.2021.125021

[51] T. Gupta, S. Siddique, R.K. Sharma, S. Chaudhary, Effect of elevated temperature and cooling regimes on mechanical and durability properties of concrete containing waste rubber fiber, Constr. Build. Mater. 137 (2019) 35–45. https://doi.org/10.1016/j.conbuildmat.2017.01.080

[52] Z. Xu, Z. Li, H. Ma, Hybrid fiber reinforced high performance concrete: mechanical properties, constitutive model and effect of fiber volume fraction, Constr. Build. Mater. 263 (2020) 120621. https://doi.org/10.1016/j.conbuildmat.2020.120621

[53] F. Aslani, M. Bastami, Constitutive relationships for normal- and high-strength concrete at elevated temperatures, ACI Mater. J. 108 (2022) 355–364. https://doi.org/10.14359/51682906